Macromolecules

Article

Cite This: Macromolecules XXXX, XXX, XXX−XXX

# Pillar[5]arene-Based Organometallic Cross-Linked Polymer: Synthesis, Structure Characterization, and Catalytic Activity in the Suzuki−Miyaura Coupling Reaction

Yuezhou Liu, Baohui Lou, Liqing Shangguan, Jingsong Cai, Huangtianzhi Zhu, and Bingbing Shi*

Department of Chemistry, Zhejiang University, Hangzhou 310027, P. R. China

*Supporting Information*

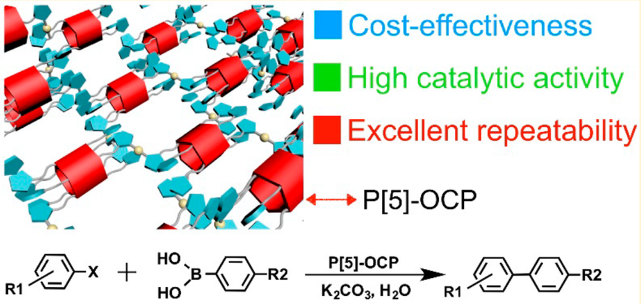

**ABSTRACT:** Heterogeneous catalysts, as an emerging research hotspot, have showed excellent advantages on stability, recyclability, and separation from reactant compared with homogeneous catalysts in recent years. Herein, pillar[5]-arene-based organometallic cross-linked polymer (**P[5]-OCP**) was constructed via the complexation between imidazolium-derivatived pillar[5]arene (**P[5]**) and $Pd(OAc)_2$. The chemical compositions and structure of the **P[5]-OCP** were confirmed by means of multiple characterization methods. The catalytic activity and process of **P[5]-OCP** were emphatically investigated in the Suzuki−Miyaura coupling reaction. The **P[5]-OCP** showed outstanding catalytic activity in mild reaction conditions. Meanwhile, the catalyst **P[5]-OCP** possessed excellent stability and recyclability, which could be reused at least five times without significant loss of activity. Furthermore, the **P[5]-OCP** is easily synthesized and cost-effective, which make it a candidate for applications in fine chemical engineering.

## INTRODUCTION

In 2010, the Nobel Prize in Chemistry was awarded collectively to Richard F. Heck, Ei-ichi Negishi, and Akira Suzuki for their great contributions to palladium-catalyzed cross-couplings in organic synthesis. Palladium-catalyzed carbon−carbon coupling reactions between aryl halides and arylboronic acids, which are very crucial methods to construct biaryl units in organic synthesis,[1] are the most powerful and general tools for the synthesis of herbicides, pharmaceuticals, natural products, liquid crystalline materials, and conducting polymers.[2,3] In the past decade, significant progress has been achieved in the constructing biaryl units by using palladium-based catalysts, especially using palladium-based homogeneous catalysts with high activities and broad substrate scopes.[4,5] However, some disadvantages of palladium-based homogeneous catalysts, such as complicated synthesis, hard separation, and intricate recycling, definitely hindered the development of palladium-based homogeneous catalysts in industry.[6,7] Compared with palladium-based homogeneous catalysts, palladium-based heterogeneous catalysts which are generally prepared by immobilizing catalytic activity sites on solid supports, porous materials, and polymers have shown remarkable advantages in stability, recyclability, and separation from the reactant.[8−10] The key characteristics of palladium-based heterogeneous catalysts are the intrinsic robustness and recyclability that satisfy wide applications in both academia and industry. Therefore, finding convenient methods and building blocks to prepare efficient palladium-based heterogeneous catalysts has consequently become a research hotspot in recent years.[11,12]

Pillar[*n*]arenes are new symmetrical calixarenes analogues, which were first discovered by Ogoshi and co-workers in 2008.[13] Pillar[*n*]arenes, as an emerging macrocyclic host, are composed of *n* hydroquinone units held together by methylene bridges linking the para positions in cyclic arrays, and the unique structure endows pillar[*n*]arenes with easy functionalization properties in supramolecular chemistry and material chemistry.[14−28] The synthesis process of pillar[*n*]arenes is efficient and low-cost, which makes pillar[*n*]arenes more suitable to construct functional materials, such as polymeric materials,[29,30] self-assembly materials,[31,32] metal−organic frameworks (MOFs),[33] supramolecular organic frameworks (SOFs),[34] and hybrid materials.[35] Nevertheless, employing pillararene-based polymer materials in heterogeneous catalysis has rarely been explored. Therefore, pillararene-based polymer materials are the emerging candidates for challenging problems in efficient heterogeneous catalytic field.

Inspired by the unique pillar-shaped and rigid structure of pillar[5]arene, here we cross-linked imidazolium-derivatived pillar[5]arene (**P[5]**) with $Pd(OAc)_2$ to construct an organometallic cross-linked polymer by using the "bottom-up" approach.[36] The metal ions ($Pd^{2+}$) were successfully immobilized and dispersed in the cross-linked polymer by the complexation between the imidazolium groups on **P[5]** and palladium ions. Then, we investigated the catalytic activity of

**Received:** December 21, 2017
**Revised:** January 28, 2018

DOI: 10.1021/acs.macromol.7b02701

Scheme 1. P[5]-OCP Derived from the Complexation between P[5] and Pd(OAc)$_2$ and Cartoon Representation of the Cross-Linked Structure of the P[5]-OCP

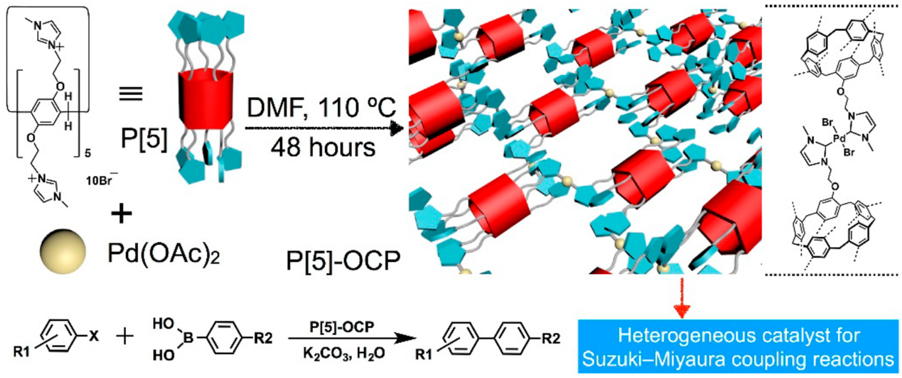

**P[5]-OCP** in the Suzuki–Miyaura coupling reaction. In this technique, water was used as solvent in the mild conditions, and the catalyst showed excellent catalytic capacity. Furthermore, **P[5]-OCP** possessed excellent stability and recyclability, which could be reused at least five times without significant loss of activity. The easy and cost-effective construction of this heterogeneous catalyst (**P[5]-OCP**) makes it candidate for applications in fine chemical engineering.

## EXPERIMENTAL SECTION

**Materials and Instrumentation.** All reagents were commercially available and used as supplied without further purification. $^1$H NMR and $^{13}$C NMR spectra were recorded with a Bruker Avance DMX 400 spectrophotometer with use of the deuterated solvent as the lock and the residual solvent or TMS as the internal reference. Scanning electron microscopy investigations were carried out on a JEOL 6390LV instrument. SEM samples were prepared by dispersing **P[5]-OCP** in DMSO via the vacuum freeze-drying methodology. Fourier transform infrared spectroscopy spectra were recorded on a Thermo Nicolet iS10 spectrometer. Transmission electron microscopic investigations were carried out on a Hitachi HT-7700 instrument. Solid-state NMR spectra were recorded on a Bruker 400WB AVANCE III spectrometer. Elemental analyses were carried out on a EA1112 instrument. Thermogravimetric analysis was carried out on a DSCQ1000 thermal gravimetric analyzer. Diffuse reflectance Fourier transform infrared (DRIFT) spectra of adsorbed CO were obtained on a Tensor 27 spectrometer (Bruker) equipped with a liquid-nitrogen-cooled mercury–cadmium–tellurium detector, a diffuse reflectance accessory, and a high-temperature reaction chamber. GC measurements were carried out using an Agilent 7890B instrument configured with an FID detector and a DB-624 column.

**Synthesis of 2.** The synthetic route of **P[5]** is shown in the Supporting Information (Scheme S1). A solution of **1** (6.74 g, 23.0 mmol) and paraformaldehyde (0.70 g, 23.0 mmol) in 1,2-dichloroethane (150 mL) was stirred vigorously at room temperature. Then boron trifluoride diethyl etherate (6.52 g, 46.0 mmol) was added to the solution, and the mixture was stirred at room temperature for 1 h. Methyl alcohol (150 mL) was added to quench the reaction. The mixture was evaporated to afford the crude product, which was isolated by flash column chromatography using ethyl acetate/petroleum ether (1:100) to give **2** as a white solid (3.7 g, 48%). $^1$H NMR (400 MHz, chloroform-*d*, room temperature) $\delta$ (ppm): 6.92 (s, 10H), 4.24 (t, $J$ = 5.7 Hz, 20H), 3.85 (s, 10H), 3.64 (t, $J$ = 5.6 Hz, 20H). $^{13}$C NMR (100 MHz, chloroform-*d*, room temperature) $\delta$ (ppm): 148.6, 128.0, 115.0, 67.9, 29.7, 28.4.

**Synthesis of P[5].** A mixture of **2** (3.36 g, 2.00 mmol) and *N*-methylimidazole (3.28 g, 40.0 mmol) in acetonitrile (50 mL) was stirred in a 150 mL round-bottom flask at 85 °C for 36 h to form a precipitate. After cooling, the mixture was filtrated and recrystallized from acetonitrile to give a white solid (3.20 g, 69%). $^1$H NMR (400 MHz, DMSO-$d_6$, room temperature) $\delta$ (ppm): 9.23 (s, 10H), 8.14 (s, 10H), 7.49 (s, 10H), 6.72 (s, 10H), 4.76 (s, 20H), 4.47 (s, 20H), 3.75 (s, 30H), 3.50 (s, 10H). $^{13}$C NMR (100 MHz, DMSO-$d_6$, room temperature) $\delta$ (ppm): 148.6, 136.9, 127.8, 123.3, 122.7, 66.4, 49.0, 40.1, 35.8. The solid-state $^{13}$C CPMAS NMR $\delta$ (ppm): 148.0, 137.1, 123.0, 113.5, 65.8, 49.2, 36.5, 27.8.

**Synthesis of P[5]-OCP.** To a solution of compound **P[5]** (1.00 g, 0.40 mmol), palladium acetate (0.45 g, 2.00 mmol) in DMF (20 mL) was stirred vigorously at 110 °C under argon for 48 h. The grayish-yellow product was obtained by filtration and washed with DMF, methylbenzene, and CH$_2$Cl$_2$. Solid-state $^{13}$C CPMAS NMR $\delta$ (ppm): 177.5, 148.8, 122.2, 113.6, 66.0, 49.3, 37.1, 31.6, 28.0.

**General Procedure for the Suzuki–Miyaura Coupling Reaction.** Aryl halide (1.0 mmol), arylboronic acid (1.5 mmol), K$_2$CO$_3$ (2.0 mmol), and **P[5]-OCP** (0.5 mol % Pd) were added to 5 mL of distilled water at 80 °C. After the reaction was completed (monitored by TLC), the mixture was extracted with CH$_2$Cl$_2$ and evaluated by GC.

## RESULTS AND DISCUSSION

**Synthesis and Structure Characterization.** The synthetic route of **P[5]-OCP** is depicted in Scheme 1. **P[5]**, which was prepared based on our previous work,[37] was selected as the rigid scaffold for the preparation of the cross-linked polymer. And then, **P[5]** was treated with Pd(OAc)$_2$ in *N*,*N*-dimethylformamide (DMF) at 110 °C for 48 h. The solid was formed on the bottom of the glassware and washed with DMF, methylbenzene, and dichloromethane to get the polymer **P[5]-OCP** as a grayish-yellow solid.

To get the information on the chemical components of the **P[5]-OCP**, elemental analysis (EA) by combustion was conducted (Figure S6). The observed contents of carbon (35.73 wt %), nitrogen (9.03 wt %), and hydrogen (4.14 wt %) in the **P[5]-OCP** matched well with the calculated values of for [(C$_{19}$H$_{22}$N$_4$O$_2$PdBr$_2$)$_n$] (C 37.56, N 9.22, H 4.15 wt %), which clearly supported the formation of the cross-linked polymer. On the other hand, the result of inductively coupled plasma atomic emission spectrum (ICP) showed that the content of palladium in **P[5]-OCP** is 17.12 wt %, corresponding to the theoretical value of 17.60 wt %.

In order to further confirm the structure of **P[5]-OCP**, $^{13}$C cross-polarization at magic angle spin (CPMAS) spectra and solid Fourier transform infrared spectroscopy (FT-IR) spectra experiments were carried out. As shown in Figure 1, in the solid-state $^{13}$C CPMAS NMR spectra of **P[5]-OCP**, all the signals of the peaks can be clearly assignable to the corresponding carbon atoms in the expected structure. In particular, the signals of the peaks at $\delta$ = 137.1 and 177.5 ppm

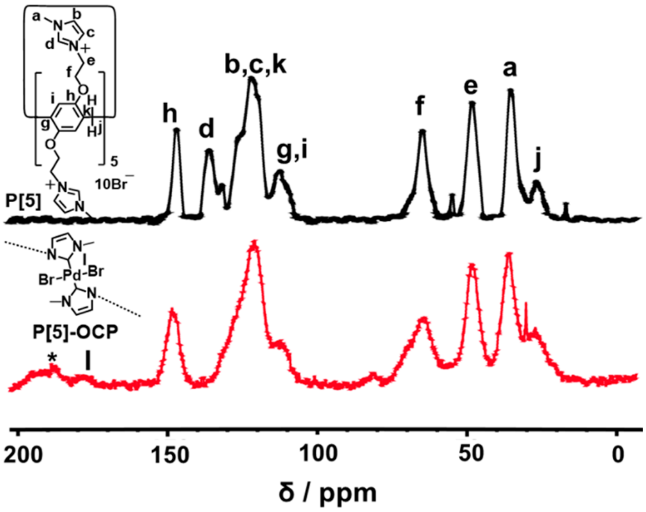

**Figure 1.** Solid-state $^{13}$C CPMAS NMR spectra of **P[5]** and **P[5]-OCP**.

can be assigned to the carbon atom d on imidazole groups of **P[5]** and carbene carbon atom l connected to the palladium atom. The disappeared signal of carbon atom d and the emerging signal of l provided the straightforward evidence for the formation of the cross-linked polymer **P[5]-OCP**. In addition, the structure of **P[5]-OCP** was further verified by solid FT-IR spectra. As shown in Figure S7, the main peaks related to **P[5]** and **P[5]-OCP** were marked and assigned. Initially, compound **P[5]** showed strong absorbance bands including O−C, Ar−C, and C═C of the benzene rings and N═C stretching vibrations at 1057, 1201, 1391−1502, and 1634 cm$^{-1}$, respectively. Compared with the peaks of compound **P[5]**, the adsorption peak of **P[5]-OCP** at 1661 cm$^{-1}$ is due to the C═C stretching vibrations, indicating the cross-linking reaction between **P[5]** and Pd(OAc)$_2$.

Scanning electron microscopy (SEM) and transmission electron microscopy (TEM) were further utilized to investigate the micromorphology of **P[5]-OCP**. The results of SEM and TEM showed that the cross-linked polymer adopted an irregular spherical shape with the size of 105 nm. The powder X-ray diffraction spectrum (XRD) experiment is usually used to analyze materials in a crystalline or noncrystalline state. In order to have a deeper sight into **P[5]-OCP**, the XRD experiment was also carried out at 298 K. As shown in Figure S8, the broad peak at 40° indicated the noncrystalline structure of **P[5]-OCP**. Furthermore, the thermogravimetric analysis (TGA) of **P[5]-OCP** (Figure S9) showed that it is stable up to 309 °C under a nitrogen atmosphere, indicating the excellent thermostability of the cross-linked polymer **P[5]-OCP**.

In order to gain the oxidation states of Pd species in **P[5]-OCP**, X-ray photoelectron spectroscopy (XPS) measurements of Pd(OAc)$_2$ and **P[5]-OCP** were carried out. As shown in Figure 3, the XPS spectra of **P[5]-OCP** contained two main peaks with binding energies of 336.8 and 342.0 eV, assignable to Pd 3d$_{5/2}$ and Pd 3d$_{3/2}$, indicating that no Pd(0) is present in **P[5]-OCP**, and the Pd species is only in the +2 state. In addition, the binding energy 336.8 eV in **P[5]-OCP** shifted negatively by 1.7 eV in comparison with that of 338.5 eV for Pd(OAc)$_2$, which indicated the strong coordination between **P[5]** and Pd$^{2+}$.[38]

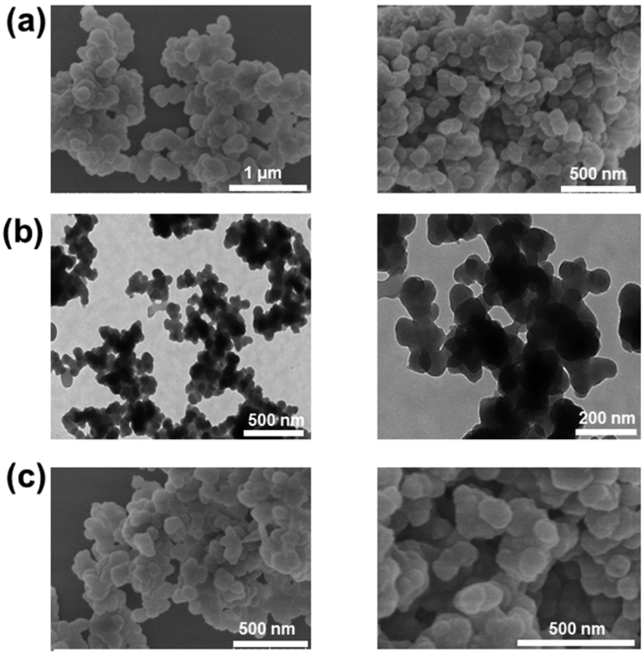

**Figure 2.** (a) SEM images of **P[5]-OCP**. (b) TEM images of **P[5]-OCP**. (c) SEM images of **P[5]-OCP** recycled after five times of the Suzuki−Miyaura coupling reaction.

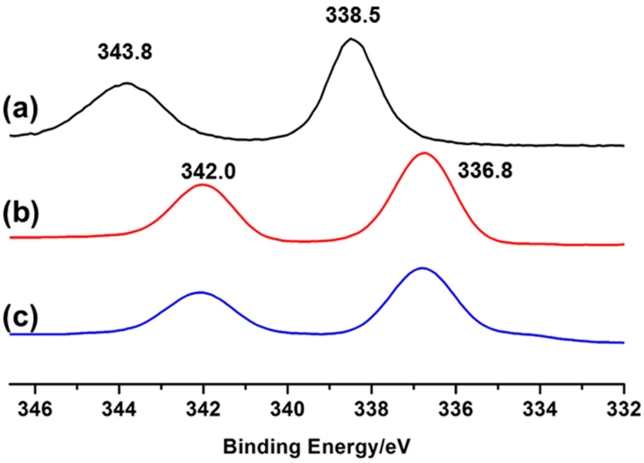

**Figure 3.** XPS analysis for Pd 3d spectra: (a) Pd(OAc)$_2$; (b) **P[5]-OCP**; (c) **P[5]-OCP** recycled after five times of the Suzuki−Miyaura coupling reaction.

In order to further study the dispersity of palladium in the polymer **P[5]-OCP**, the CO-absorbed diffuse reflectance Fourier transform infrared (DRIFT) spectra experiment for **P[5]-OCP** was performed (Figure 4). The bands at 2152 and 2129 cm$^{-1}$ are ascribed to CO, which is linearly adsorbed on Pd. The band at 1889 cm$^{-1}$ is ascribed to the bridge-bond CO on two Pd atoms and CO adsorbed between Pd clusters. The intensity of bridge-bound CO relative to linear-bound CO of **P[5]-OCP** is determined as 0.19, suggesting the high dispersity of palladium in the polymer, which contributed to the reaction process as a catalyst.[38]

**Catalytic Activities.** Palladium-catalyzed carbon−carbon coupling reactions between aryl halides and arylboronic acids are very crucial methods to construct biaryl units in organic synthesis. In order to investigate the catalytic activities of **P[5]-OCP**, Suzuki−Miyaura coupling reaction between aryl halides and arylboronic acids was evaluated in the presence of **P[5]-OCP** and K$_2$CO$_3$ in H$_2$O at 80 °C. Herein, we chose water as

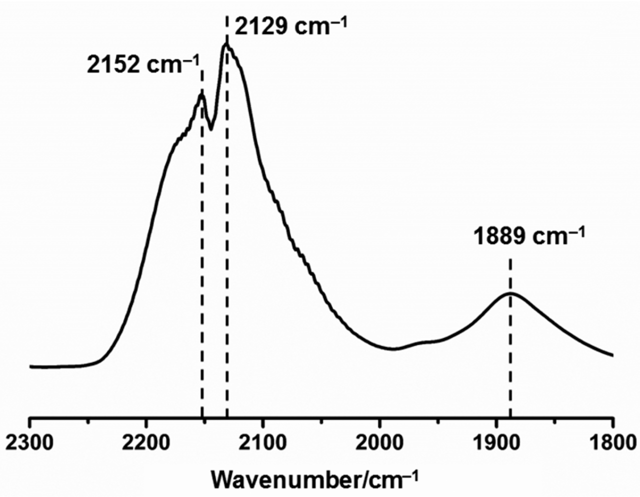

**Figure 4.** DRIFT spectra of CO absorbed at 25 °C on **P[5]-OCP**.

solvent for the Suzuki−Miyaura coupling reaction because water is a green solvent and nontoxic.

Table 1 summarizes the catalytic activity of **P[5]-OCP** toward a variety of aryl halides and arylboronic acids. The different substrates, including electron-donating and electron-withdrawing compounds, were tested in the Suzuki−Miyaura coupling reactions, giving the corresponding biaryls in excellent yields. Moreover, in the previous work, aryl chlorides have low reaction activity in the Suzuki−Miyaura reaction catalyzed by most of the present heterogeneous palladium catalysts.[12] Herein, the catalyst **P[5]-OCP** was also used in these highly challenging substrates. Particularly, the less active aryl chlorides also gave good yields (100, 80.0, and 91.4%) with longer reaction time (12 h, entries 18−20), indicating the catalyst has excellent catalytic activity and universality.

**Table 1. Suzuki−Miyaura Coupling Reactions Catalyzed by P[5]-OCP**

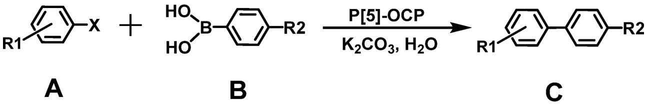

| entry | X | R1 | R2 | $T$ (h) | yield[a,b] (%) |
|---|---|---|---|---|---|
| 1 | I | H | H | 1 | 100 |
| 2 | I | *p*-$OCH_3$ | H | 1 | 100 |
| 3 | I | *p*-$NO_2$ | H | 2 | 100 |
| 4 | Br | H | H | 2 | 100 |
| 5 | Br | H | $CH_3$ | 6 | 74.3 |
| 6 | Br | H | $OCH_3$ | 6 | 81.1 |
| 7 | Br | *p*-$OCH_3$ | H | 6 | 100 |
| 8 | Br | *p*-$OCH_3$ | $CH_3$ | 6 | 82.6 |
| 9 | Br | *p*-$OCH_3$ | $OCH_3$ | 6 | 100 |
| 10 | Br | *p*-CN | H | 6 | 95.3 |
| 11 | Br | *p*-CN | $CH_3$ | 6 | 88.0 |
| 12 | Br | *p*-CN | $OCH_3$ | 6 | 96.3 |
| 13 | Br | *p*-$CH_3$ | H | 6 | 86.6 |
| 14 | Br | *p*-$NO_2$ | H | 8 | 73.9 |
| 15 | Br | *p*-CHO | H | 6 | 91.5 |
| 16 | Br | *m*-CHO | H | 6 | 90.9 |
| 17 | Br | *o*-CHO | H | 6 | 91.6 |
| 18 | Cl | H | H | 12 | 100 |
| 19 | Cl | *p*-$OCH_3$ | H | 12 | 80.0 |
| 20 | Cl | *m*-CHO | H | 12 | 91.4 |
| 21 | Br | H | H | 2 | 100[c] |
| 22 | Br | H | H | 2 | 80.6[d] |
| 23 | Br | *p*-$C(CH_3)_3$ | H | 6 | 67.4 |
| 24 | Br | H | H | 2 | 78.9[e] |

[a] Reaction conditions: aryl halide (1.0 mmol), arylboronic acid (1.5 mmol), $K_2CO_3$ (2.0 mmol), **P[5]-OCP** (0.5 mol % Pd), $H_2O$ (5 mL), 80 °C. [b] Yield were determined by GC/MS. [c] The reaction was performed in the presence of Hg. [d] The reaction was performed in the presence of P4VP. [e] The reaction was performed in the presence of adiponitrile.

In order to demonstrate the importance of **P[5]** for the reaction, an attempt to study the interaction between **P[5]** and bromobenzene was carried out by $^1H$ NMR characterization (Figure S10). The resulting $^1H$ NMR spectrum showed that obvious upfield shifts in the signals of all the protons from bromobenzene while the signals of protons of **P[5]** shifted downfield, indicating that bromobenzene was encapsulated into the cavity of **P[5]**. These facts suggested that the high yield was attributable to the host−guest interaction between the **P[5]** and aryl halide, which enhances the interaction between reagents and palladium. As control experiments, 1-bromo-4-*tert*-butylbenzene was chosen as reactant which cannot enter into the cavity of **P[5]**. As expected, the yield decreased when the substrates possessed bulky substituents (entry 23), indicating that the substrates with bulky substituents have negative effect on the reaction. On the other hand, adiponitrile can be used as competitive guest due to the strong complexation with pillararene. As shown in the table, the yield of the reaction of bromobenzene and phenylboronic acid was nearly 100%, while the yield dropped to 78.9% in the same reaction condition except the excess adiponitrile, indicating the importance of the host−guest interaction between the **P[5]** and aryl halide.

To make sure whether the catalyst **P[5]-OCP** is practically working in a heterogeneous pathway, or whether it is only a precatalyst for more active soluble species, a series of different control tests have been carried out.[39] First, the hot-filtration test was conducted by using **P[5]-OCP** as a catalyst. In the absence of the reactant, the mixture of **P[5]-OCP** and $K_2CO_3$ in distilled water was heated for 1 h at 80 °C. Then the filtrate from the mixture was used to catalyze the reaction of bromobenzene and phenylboronic acid, but no coupling product was observed. Next, when the reaction of bromobenzene and phenylboronic acid was proceeded for about 20 min in the presence of **P[5]-OCP**, the conversion of bromobenzene reached about 60.79%. The reaction was allowed to react another 100 min after removing the catalyst, but no distinct progress (1.90% by GC) was observed. However, it was not powerful evidence to prove that the catalytic activity of **P[5]-OCP** was performed in a heterogeneous way because the leached and soluble Pd species could be redepositing back on the polymer backbone during the hot filtration. So, mercury poisoning test was also employed to explore the catalytic process of bromobenzene and phenylboronic acid. Interestingly, as one drop of Hg was added in the reaction, the yield is up to 100%, which provided the proof that **P[5]-OCP** is not a precatalyst for the formation of Pd nanoparticles. In addition, poly(4-vinylpyridine) (P4VP), an efficient poison for the Pd-catalyzed Suzuki coupling reaction, was also used to ascertain the reaction process. Then, the coupling reaction of bromobenzene and phenylboronic acid was carried out in the presence of P4VP (P4VP/Pd 400:1). It is

DOI: 10.1021/acs.macromol.7b02701

noteworthy that this new control experiment give biphenyl in 80.6% conversion after 2 h at 60 °C, leading to a gradual decrease in catalytic activity of **P[5]-OCP**. Thus, the current measurements clearly indicated that catalyst **P[5]-OCP** is partly operating in an incompletely heterogeneous pathway.

The stability and reusability are very important factors of catalysts. The excellent catalytic activity of **P[5]-OCP** encouraged us to investigate its recyclability. The recycled use of **P[5]-OCP** was examined in the reaction of bromobenzene and phenylboronic acid. After the end of the reaction, **P[5]-OCP** was isolated through simple extraction, dried in vacuo, and then employed for the next run. It was found that the recycling can be successfully achieved in five reaction runs and no detectable loss in performence (Figure 5). In agreement with the results from reusability studies, the XPS analysis confirms that no significant degradation of Pd nanoparticles (via oxidation) occurs over the course of the catalytic reaction after looping five times (Figure 3c). Meanwhile, the spherical shape of the catalyst did not show any significant changes after five times cycling based on the SEM images (Figure 2c). Furthermore, we supplemented the $^{13}$C CPMAS NMR and FT-IR of **P[5]-OCP** recycled after five times of the Suzuki–Miyaura coupling reaction. Compared with **P[5]-OCP** freshly prepared, the spectra did not show any significant changes after five times cycling, which provided a direct evidence that the **P[5]-OCP** possessed excellent stability in the recycling processes.

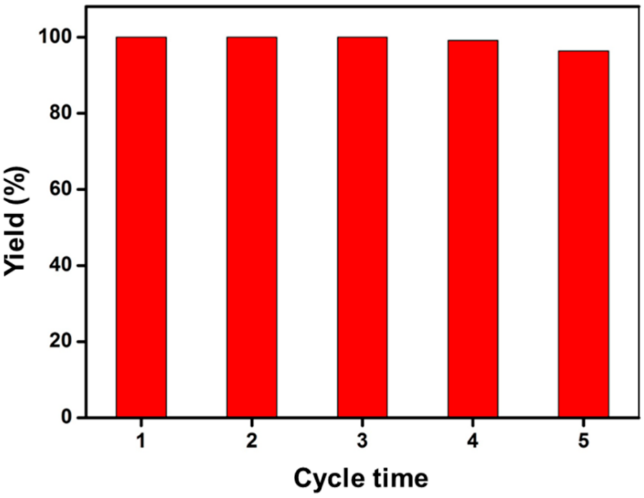

**Figure 5.** Reusability of the **P[5]-OCP** catalyst in the Suzuki–Miyaura coupling reaction.

## CONCLUSION

Organometallic cross-linked polymer **P[5]-OCP** was prepared based on the complexation between **P[5]** and Pd(OAc)$_2$. The cross-linked structure of the polymer **P[5]-OCP** was analyzed by solid-state $^{13}$C CPMAS NMR, FT-IR, electron microscopy, EA, ICP, and XPS. The result of DRIFT spectra experiment indicated the high dispersity of palladium in **P[5]-OCP**. The **P[5]-OCP** demonstrated excellent activity in a serious of Suzuki–Miyaura coupling reactions. The catalyst can be reused at least five times without significant loss of activity, indicating the outstanding stability and reusability. This cross-linked polymer can extend the development of heterogeneous catalysts because of its cost-effectiveness, high catalytic activity, and recycling potential. Furthermore, this work can provide a new perspective to introduce pillararenes into functional materials and enrich the field of material science and supramolecular chemistry.

## ASSOCIATED CONTENT

### Supporting Information

The Supporting Information is available free of charge on the ACS Publications website at DOI: 10.1021/acs.macromol.7b02701.

Additional NMR and FT-IR spectra, thermogravimetric analyses, XRD and GC/MS spectra (PDF)

## AUTHOR INFORMATION

### Corresponding Author

*E-mail: bingbingshi@zju.edu.cn (B.S.).

### ORCID

Bingbing Shi: 0000-0001-9523-5758

### Notes

The authors declare no competing financial interest.

## ACKNOWLEDGMENTS

We thank Jie Fan from Zhejiang University for the support of DRIFT spectra experiment for **P[5]-OCP**. This work was supported by the Fundamental Research Funds for the Central Universities.

## REFERENCES

(1) Corbet, J.-P.; Mignani, G. Selected Patented Cross-Coupling Reaction Technologies. *Chem. Rev.* **2006**, *106*, 2651–2710.

(2) Miyaura, N.; Suzuki, A. Palladium-Catalyzed Cross-Coupling Reactions of Organoboron Compounds. *Chem. Rev.* **1995**, *95*, 2457–2483.

(3) Hassan, J.; Sevignon, M.; Gozzi, C.; Schulz, E.; Lemaire, M. Aryl–Aryl Bond Formation One Century after the Discovery of the Ullmann Reaction. *Chem. Rev.* **2002**, *102*, 1359–1470.

(4) Zhang, G.; Peng, Y.; Cui, L.; Zhang, L. Gold-Catalyzed Homogeneous Oxidative Cross-Coupling Reactions. *Angew. Chem., Int. Ed.* **2009**, *48*, 3112–3115.

(5) Erdélyi, M.; Gogoll, A. Rapid Homogeneous-Phase Sonogashira Coupling Reactions Using Controlled Microwave Heating. *J. Org. Chem.* **2001**, *66*, 4165–4169.

(6) Lin, M.; Wang, S.; Zhang, J.; Luo, W.; Liu, H.; Wang, W.; Su, C. Guest Uptake and Heterogeneous Catalysis of a Porous Pd(II) *N*-Heterocyclic Carbene Polymer. *J. Mol. Catal. A: Chem.* **2014**, *394*, 33–39.

(7) Ranganath, K. V. S.; Onitsuka, S.; Kumar, A. K.; Inanaga, J. Recent Progress of *N*-Heterocyclic Carbenes in Heterogeneous Catalysis. *Catal. Sci. Technol.* **2013**, *3*, 2161–2181.

(8) Wang, Z.; Chen, G.; Ding, K. Self-Supported Catalysts. *Chem. Rev.* **2009**, *109*, 322–359.

(9) Xu, S.; Song, K.; Li, T.; Tan, B. Palladium Catalyst Coordinated in Knitting *N*-Heterocyclic Carbene Porous Polymers for Efficient Suzuki–Miyaura Coupling Reactions. *J. Mater. Chem. A* **2015**, *3*, 1272–1278.

(10) Sangtrirutnugul, P.; Chaiprasert, T.; Hunsiri, W.; Jitjaroendee, T.; Songkhum, P.; Laohhasurayotin, K.; Osotchan, T.; Ervithayasuporn, V. Tunable Porosity of Cross-Linked-Polyhedral Oligomeric Silsesquioxane Supports for Palladium-Catalyzed Aerobic Alcohol Oxidation in Water. *ACS Appl. Mater. Interfaces* **2017**, *9*, 12812–12822.

(11) Zhang, C.; Wang, J.; Liu, Y.; Ma, H.; Yang, X.; Xu, H. Main-Chain Organometallic Microporous Polymers Based on Triptycene: Synthesis and Catalytic Application in the Suzuki–Miyaura Coupling Reaction. *Chem. - Eur. J.* **2013**, *19*, 5004–5008.

(12) Wang, C.; Li, Y.; Hou, X.; Han, Y.; Nie, K.; Zhang, J. *N*-Heterocyclic Carbene-based Microporous Organic Polymer Supported Palladium Catalyst for Carbon-Carbon Coupling Reaction. *ChemistrySelect.* **2016**, *1*, 1371−1376.

(13) Ogoshi, T.; Kanai, S.; Fujinami, S.; Yamagishi, T. A.; Nakamoto, Y. *para*-Bridged Symmetrical Pillar[5]arenes: Their Lewis Acid Catalyzed Synthesis and Host−Guest Property. *J. Am. Chem. Soc.* **2008**, *130*, 5022−5023.

(14) Cao, D.; Kou, Y.; Liang, J.; Chen, Z.; Wang, L.; Meier, H. A Facile and Efficient Preparation of Pillararenes and a Pillarquinone. *Angew. Chem., Int. Ed.* **2009**, *48*, 9721−9723.

(15) Ogoshi, T.; Kayama, H.; Yamafuji, D.; Aoki, T.; Yamagishi, T. Supramolecular Polymers with Alternating Pillar[5]arene and Pillar[6]arene Units from a Highly Selective Multiple Host−Guest Complexation System and Monofunctionalized Pillar[6]arene. *Chem. Sci.* **2012**, *3*, 3221−3226.

(16) Ji, X.-F.; Xia, D.-Y.; Yan, X.; Wang, H.; Huang, F.-H. Supramolecular Polymer Materials Based on Crown Ether and Pillararene Host-Guest Recognition Motifs. *Acta Polym. Sin.* **2017**, 9−18.

(17) Hu, X.-B.; Chen, L.; Si, W.; Yu, Y.; Hou, J.-L. Pillar[5]arene Decaamine: Synthesis, Encapsulation of Very Long Linear Diacids and Formation of Ion Pair-Stopped [2]Rotaxanes. *Chem. Commun.* **2011**, *47*, 4694−4696.

(18) Zhang, Y.-M.; Shi, B.-B.; Li, H.; Qu, W.-J.; Gao, G.-Y.; Lin, Q.; Yao, H.; Wei, T.-B. Copillar[5]arene-based Supramolecular Polymer Gels. *Polym. Chem.* **2014**, *5*, 4722−4725.

(19) Yuan, B.; Xu, J.-F.; Sun, C.-L.; Nicolas, H.; Schönhoff, M.; Yang, Q.-Z.; Zhang, X. Pillar[6]arene Containing Multilayer Films: Reversible Uptake and Release of Guest Molecules with Methyl Viologen Moieties. *ACS Appl. Mater. Interfaces* **2016**, *8*, 3679−3685.

(20) Li, C. Pillararene-based Supramolecular Polymers: from Molecular Recognition to Polymeric Aggregates. *Chem. Commun.* **2014**, *50*, 12420−12433.

(21) Li, C.; Han, K.; Li, J.; Zhang, H.; Ma, J.; Shu, X.; Chen, Z.; Weng, L.; Jia, X. Synthesis of Pillar[5]arene Dimers and Their Cooperative Binding toward Some Neutral Guests. *Org. Lett.* **2012**, *14*, 42−45.

(22) Hu, X.-B; Chen, Z.; Tang, G.; Hou, J.-L; Li, Z.-T. Single-Molecular Artificial Transmembrane Water Channels. *J. Am. Chem. Soc.* **2012**, *134*, 8384−8387.

(23) Si, W.; Chen, L.; Hu, X.-B; Chen, Z.; Hou, J.-L; Li, Z.-T. Selective Artificial Transmembrane Channels for Protons by Formation of Water Wires. *Angew. Chem.* **2011**, *123*, 12772−12776.

(24) Wu, J.; Sun, S.; Feng, X.; Shi, J.; Hu, X.-Y; Wang, L. Controllable Aggregation-induced Emission based on a Tetraphenylethylene-functionalized Pillar[5]arene via Host−Guest Recognition. *Chem. Commun.* **2014**, *50*, 9122−9125.

(25) Lin, Q.; Zhong, K.-P; Zhu, J.-H; Ding, L.; Su, J.-X; Yao, H.; Wei, T.-B; Zhang, Y.-M. Iodine Controlled Pillar[5]arene-Based Multiresponsive Supramolecular Polymer for Fluorescence Detection of Cyanide, Mercury, and Cysteine. *Macromolecules* **2017**, *50*, 7863−7871.

(26) Liu, Y.; Shangguan, L.; Wang, H.; Xia, D.; Shi, B. A Supramolecular Polymer Network Gel with Stimuli-Responsiveness Constructed by Orthogonal Metal Ion Coordination and Pillar[5]-arene-based Host−Guest Recognition. *Polym. Chem.* **2017**, *8*, 3783−3787.

(27) Liao, X.; Guo, L.; Chang, J.; Liu, S.; Xie, M.; Chen, G. Thermoresponsive AuNPs Stabilized by Pillararene-Containing Polymers. *Macromol. Rapid Commun.* **2015**, *36*, 1492−1497.

(28) Chang, J.; Zhao, Q.; Kang, L.; Li, H.; Xie, M.; Liao, X. Multiresponsive Supramolecular Gel Based on Pillararene-Containing Polymers. *Macromolecules* **2016**, *49*, 2814−2820.

(29) Shi, B.; Xia, D.; Yao, Y. A Water-Soluble Supramolecular Polymer Constructed by Pillar[5]arene-based Molecular Recognition. *Chem. Commun.* **2014**, *50*, 13932−13935.

(30) Shi, B.; Jie, K.; Zhou, Y.; Xia, D.; Yao, Y. Formation of Fluorescent Supramolecular Polymeric Assemblies via Orthogonal Pillar[5]arene-based Molecular Recognition and Metal Ion Coordination. *Chem. Commun.* **2015**, *51*, 4503−4506.

(31) Duan, Q.; Cao, Y.; Li, Y.; Hu, X.; Xiao, T.; Lin, C.; Pan, Y.; Wang, L. pH-Responsive Supramolecular Vesicles Based on Water-Soluble Pillar[6]arene and Ferrocene Derivative for Drug Delivery. *J. Am. Chem. Soc.* **2013**, *135*, 10542−10549.

(32) Shi, B.; Jie, K.; Zhou, Y.; Zhou, J.; Xia, D.; Huang, F. Nanoparticles with Near-Infrared Emission Enhanced by Pillararene-Based Molecular Recognition in Water. *J. Am. Chem. Soc.* **2016**, *138*, 80−83.

(33) Strutt, N. L.; Fairen-Jimenez, D.; Iehl, J.; Lalonde, M. B.; Snurr, R. Q.; Farha, O. K.; Hupp, J. T.; Stoddart, J. F. Incorporation of an A1/A2-Difunctionalized Pillar[5]arene into a Metal−Organic Framework. *J. Am. Chem. Soc.* **2012**, *134*, 17436−17439.

(34) Tan, L.-L.; Li, H.; Tao, Y.; Zhang, S. X.-A.; Wang, B.; Yang, Y.-W. Pillar[5]arene-Based Supramolecular Organic Frameworks for Highly Selective $CO_2$-Capture at Ambient Conditions. *Adv. Mater.* **2014**, *26*, 7027−7031.

(35) Li, H.; Chen, D.-X.; Sun, Y.-L.; Zheng, Y.-B.; Tan, L.-L.; Weiss, P. S.; Yang, Y.-W. Viologen-Mediated Assembly of and Sensing with Carboxylatopillar[5]arene-Modified Gold Nanoparticles. *J. Am. Chem. Soc.* **2013**, *135*, 1570−1576.

(36) Mijatovic, D.; Eijkel, J. C. T.; van den Berg, A. V. D. Technologies for Nanofluidic Systems: Top-Down vs. Bottom-Up− a Review. *Lab Chip* **2005**, *5*, 492−500.

(37) Yao, Y.; Xue, M.; Chi, X.; Ma, Y.; He, J.; Abliz, Z.; Huang, F. A New Water-Soluble Pillar[5]arene: Synthesis and Application in the Preparation of Gold Nanoparticles. *Chem. Commun.* **2012**, *48*, 6505−6507.

(38) Chen, Y.; Wang, H.; Liu, C.-J.; Zeng, Z.; Zhang, H.; Zhou, C.; Jia, X.; Yang, Y. Formation of Monometallic Au and Pd and Bimetallic Au−Pd Nanoparticles Confined in Mesopores via Ar Glow-Discharge Plasma Reduction and Their Catalytic Applications in Aerobic Oxidation of Benzyl Alcohol. *J. Catal.* **2012**, *289*, 105−117.

(39) Karimi, B.; Akhavan, P. F. A Study on Applications of N-Substituted Main-Chain NHC-Palladium Polymers as Recyclable Self-Supported Catalysts for the Suzuki−Miyaura Coupling of Aryl Chlorides in Water. *Inorg. Chem.* **2011**, *50*, 6063−6072.

DOI: 10.1021/acs.macromol.7b02701
*Macromolecules* XXXX, XXX, XXX−XXX